Proceedings of the ASME 2010 Conference on Smart Materials, Adaptive Structures and Intelligent Systems
SMASIS2010
September 28 – October 1, 2010, Philadelphia, Pennsylvania, USA

SMASIS2010-3838

A PROBABILISTIC MODEL UPDATING ALGORITHM FOR FATIGUE DAMAGE DETECTION IN ALUMINUM HULL STRUCTURES

Masahiro Kurata Jun-Hee Kim Jerome P. Lynch
Department of Civil and Environmental Engineering, University of Michigan, Ann Arbor, MI

Kincho H. Law
Department of Civil and Environmental Engineering, Stanford University, Stanford, CA

Liming W. Salvino
Structures and Composite Carderock Division, Naval Surface Warfare Center, West Bethesda, MD

ABSTRACT

The use of aluminum alloys in the design of naval structures offers the benefit of light-weight ships that can travel at high-speed. However, the use of aluminum poses a number of challenges for the naval engineering community including higher incidence of fatigue-related cracks. Early detection of fatigue induced cracks enhances maintenance of the ships and is critical for preventing the catastrophic failure of the hull. Furthermore, monitoring the integrity of the aluminum hull can provide valuable information for estimating the residual life of hull components. This paper presents a model-based damage detection methodology for fatigue assessment of hulls that are instrumented with a long-term hull monitoring system. At the core of the data driven damage detection approach is a Bayesian model updating algorithm enhanced with systematic enumeration and pruning of candidate solutions. The Bayesian model updating approach significantly reduce the computational effort by systematically narrowing the search space using errors functions constructed using the estimated modal properties associated with the condition of the structure. This study proposes the use of the Bayesian model updating technique to detect damage in an aluminum panel modeled using high-fidelity finite element models. The performance of the proposed damage detection method is tested through simulation of a progressively growing fatigue crack introduced in the vicinity of a welded stiffener element. An experimental study verifies the accuracy of the proposed damage detection method using an aluminum plate excited with a controlled excitation in the laboratory.

INTRODUCTION

Aluminum alloys are increasingly being used as the choice of material for ship hulls, especially in high-speed vessels, where the relatively light-weight and high corrosion resistance properties of the material is attractive. However, the design and operation of ships with aluminum hulls has been fairly recent in the naval community. Long-term monitoring and evaluation of aluminum hull performance with respect to hull aging and fatigue accumulation (or related damage) is needed. Fatigue-related damage in aluminum alloys often appear as widespread micro-cracks; this is in contrast to the large-size fatigue cracks of steel alloys that lead to rapid strength deterioration of the system. While steel vessels would need immediate attention upon the initiation of fatigue cracking, high-speed aluminum hulls can remain in operation even after the initiation of micro-cracks because of the ductile mechanical characteristic of the material. However, close monitoring and evaluation of hull health has the potential to extend the operational life of high-speed aluminum vessels by ensuring micro-cracks do not nucleate into more severe cracks that undermine the hull performance.

Frequent inspection of ship hulls can extend the operational life of a ship since the detection of the onset of damage can reduce overall ship life-cycle costs. However, current visual inspections of the entire hull are both costly and labor-intensive. Therefore, the instrumentation of a structural health monitoring (SHM) system coupled with an effective damage detection methodology can reduce the cost of

inspection by providing inspectors with a prioritized list of probable areas of damage. Such a list would effectively narrow down the areas of the hull requiring detailed inspections (perhaps by conducting nondestructive testing with ultrasonic waves, *etc.*).

This study presents the development of a model-based damage detection algorithm for autonomous structural health monitoring of aluminum hull structures. The area of damage in the structure is estimated by comparing the structural characteristics of the "true" structure (damaged or undamaged) and finite element "trial" models. The probability associated with a hypothesized damage state (*e.g.*, location and size) is evaluated through the calculation of an error between the "true" and "trial" models. In the proposed algorithm, the probability distribution of the probable damage area (*i.e.*, fatigue crack path) is sharpened by repeatedly applying a Bayesian inference algorithm [1, 2]. The error distribution in the model-updating algorithm is treated as a discrete function and does not require computationally expensive integration as is commonly associated with other Bayesian analyses. To sample the posterior parameter distribution, other Bayesian approaches implemented with the Markov Chain Monte Carlo (MCMC) method and genetic algorithms (GA) were reported with successful performance in detecting structural damage detection [3-5]. However, these approaches are computationally expensive and do not always guarantee the convergence of a solution. To reduce the computational effort, the Bayesian damage detection algorithm proposed herein is enhanced with a branch-and-bound search technique where the search space is systematically narrowed through enumeration and pruning of candidate model solutions [6].

In this study, two types of error functions are constructed to estimate the error intrinsic to a hypothesized damage state. The first error function compares the model properties (modal frequency and mode shape) of the "true" and "trial" models. The second error function is based on the flexibility of the structure. The proposed model updating algorithm using both objective functions is tested numerically and later verified through experimentation using an aluminum plate with a crack intentionally introduced near a welded stiffener element.

THEORETICAL BACKGROUND AND ALGORITHM

MODEL UPDATING FOR DAMAGE DETECTION

A general class of damage detection algorithms is based on model updating [7]. In such methods, model parameters are varied until the model approximates the behavior of the true observed system. Here, changes in model parameters are correlated to the condition of the structure (damage versus undamaged). To identify an optimal model, model parameters are varied with model and observed system outputs used to evaluate an objective (or error) function. Model parameters that minimize the objective functions can be defined in both the time- and frequency-domains. An appropriate objective function is one that takes into account the fundamental behavior of the system in both its damaged and undamaged states, yet is compatible with the experimental data available.

Consider a simple plate structure. The governing equation describing the dynamic behavior of a vibrating plate can be written in the following generalized form [8]:

$$D\nabla^4 w + \rho h \frac{\partial^2 w}{\partial t^2} = q(x, y, t) \qquad \text{Eq. 1}$$

where D is the flexural rigidity and is defined as:

$$D = \frac{Eh^3}{12(1-v^2)} \qquad \text{Eq. 2}$$

Here, w denotes the vertical displacement of the plate, $q(x, y, t)$ is the normal load distribution function on the top of the plate, ρ is the plate density, h is the plate thickness, E is the Young's (elastic) modulus and v is the Poisson ratio.

For modeling purposes, fatigue crack damage can be represented by a change in the stiffness of the plate at a damage location. More specific, a crack is equivalent to a drastic reduction in the material elastic modulus in the locations of the crack. For a finite element model with N total elements, the effective elastic modulus can be expressed in discrete form as:

$$E' = \{E_1, E_2, \cdots, E_i, E_{i+1}, \cdots, E_{i+n}, \cdots, E_{N-1}, E_N\} \qquad \text{Eq. 3}$$

If the model contains n damaged elements whose effective Young's modulus in the damaged state is reduced by the factor k (< 1), then the moduli E_{i+1} through E_{i+n} would be replaced by $kE_{i+1}, \cdots, kE_{i+n}$ in Eq.3.

Model updating in the damage detection problem can be formulated as a combinatorial optimization problem that seeks to find an optimal E' that minimizes a defined objective function that compares the FEM model output using the hypothesized, E', and the output derived from actual measurements taken from the structure. This inverse problem can be posed as a combinatorial optimization problem for finding the optimal set of n elements, whose effective elastic modulus:

$$E_d = \{kE_{i+1}, \cdots, kE_{i+n-1}, kE_{i+n}\} \qquad \text{Eq. 4}$$

represents the damage state of the real structure.

BAYESIAN FORMULATION

The model updating procedure adopted is based on a Bayesian probabilistic approach which utilizes the parameters measured or estimated from collected signals or data (which may contain uncertainties and noise). Unlike a deterministic optimization formulation, the state space search must reflect the relative degree of belief on the estimates of the optimal subset (*i.e.*, E_d, in this case). Let M denote the hypothesized damage states of the model. The calculation of the error that exists between the "true" structure and the FEM "trial" model (s) is based on the measured or estimated structural parameters. The

updated estimates on the damage of the structure are expressed as the posterior distribution based on Baye's rule as follows

$$p(M|s) = \frac{p(s|M)p(M)}{p(s)} \propto p(s|M)p(M) \qquad \text{Eq. 5}$$

where $p(M|s)$ is the posterior distribution function for a hypothesis M given the measured or estimated parameters, s. $p(s|M)$ is termed the likelihood function, $p(M)$ is the prior probability of the hypothesis and $p(s)$ is treated here as some normalization constant. Therefore, by collecting the likelihood function (the objective function associate with error for the given data set), the posterior distribution $p(M|s)$ becomes a better estimate than prior probability $p(M)$ as the process goes on. For instance, if the initial estimate of the probable area of damage is assumed distributed uniformly over the structure before the application of the algorithm, the most likely damaged areas are revealed with relatively higher posterior estimates by the repeated applications of the Bayesian inference algorithm.

BRANCH AND BOUND

The selection of the most probable events from all conceivable possibilities using the Bayesian probabilistic approach can be systematized using various "optimal" search methods; otherwise a random search in optimal subspace becomes a computationally intractable task. In this study, the Branch and Bound (BB) technique is applied to reduce the search space in the model updating process. The BB technique is a general search method originally developed for discrete optimization problems and is a powerful technique for controlling the size of a search space used in model updating [6]. As illustrated in Figure 1, the BB algorithm initially starts its search from some random subspaces (*i.e.*, leaf nodes associated with Branch 1 in Figure 1). The algorithm continues to take an additional sample (*i.e.*, an additional element in the hypothesized subset) at each leaf node to improve their estimates. As the search proceeds, the branches associated with large "errors" are pruned and the search is bounded by evaluating the remaining branches. Therefore, the probable damage area in a system can be systematically narrowed by implementing the BB technique in the Bayesian formulation. Moreover, the computational effort and accuracy of the estimates for the optimal subset (*i.e.*, E_d) can be aggressively controlled by selecting an optimal pruning rate at each branch.

THE OBJECTIVE (ERROR) FUNCTIONS

The errors associated with each leaf node in the BB algorithm are evaluated using the objective functions that consider the difference in the structural characteristics of the true (damaged) structure and a trial FEM model with properties resembling the damaged structure. In this study, two objective functions based on frequency domain information (*i.e.*, modal properties) are considered. The first approach is named the "Direct Mode-Based Approach (DMBA)" and evaluates the difference in the modal properties (modal frequencies and mode shape) of the true damaged structure and the trial FEM model independently. The DMBA method then calculates the error function as the sum of the errors associated with each property. The other method is named the "Flexibility-Based Approach (FBA)" and evaluates an error function using modal properties in a combined manner using the flexibility matrix.

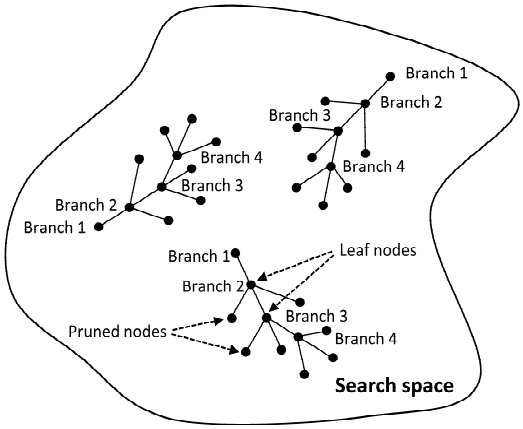

Figure 1. Branch and Bound technique.

DIRECT MODE-BASED APPROACH (DMBA)

The objective function of the DMBA, J_{DMBA}, considers a weighted combination of differences in modal frequency (ω) and mode shape (ϕ). Here, the objective function is formulated as follows:

$$J_{DMBA} = \sum_{i=1}^{n} \left(\frac{\omega_i^{true} - \omega_i^{trial}}{\omega_i^{trial}} \right)^2 + \alpha \sum_{i=1}^{n} \frac{\left(1 - \sqrt{MAC_i}\right)^2}{MAC_i} \qquad \text{Eq. 6}$$

where

$$MAC_i = \frac{\left| \left(\phi_i^{true}\right)^T \left(\phi_i^{trial}\right) \right|^2}{\left\{ \left(\phi_i^{true}\right)^T \left(\phi_i^{true}\right) \right\} \left\{ \left(\phi_i^{trial}\right)^T \left(\phi_i^{trial}\right) \right\}} \qquad \text{Eq. 7}$$

The objective function considers n modes with ω_i^{true} and ω_i^{trial} being the modal frequencies of a true structure and a trial model, respectively, for the i^{th} mode. The scalar parameter MAC_i is the modal assurance criteria (MAC) and provides a measure of correlation (with $0 \leq MAC_i \leq 1$) between the true observed i^{th} mode, ϕ_i^{true}, and the i^{th} mode of the trial model ϕ_i^{trial}, The weighting term, α, allows the objective function to weight the mode shape differences relative to the modal frequencies. The coordinates (*i.e.*, the entries) of the true and trial mode shapes are evaluated only at the locations of the sensors, based on the measurements obtained either from an experiment or an FEM simulation.

FLEXIBILITY-BASED APPROACH (FBA)

The FBA method formulates an objective function based on the difference between the flexibility matrices that correspond to the true and trial models. The inverse

relationship between the flexibility matrix and the square of modal frequency renders the flexibility matrix as less sensitive to high frequency modes. This unique characteristic allows for the inclusion of lower order modes in a truncated flexibility matrix. This feature has attracted many researchers to explore flexibility as a core element in developing structural damage detection algorithms [*e.g.*, 9-13].

When the mode shapes are mass-normalized (*i.e.*, $\bar{\Phi}^T M \bar{\Phi} = I$), the stiffness matrix K and the flexibility matrix F are related to the modal properties as follows:

$$K = M\bar{\Phi}\Omega\bar{\Phi}^T M \qquad \text{Eq. 8}$$

and

$$F = \bar{\Phi}\Omega^{-1}\bar{\Phi}^T = \sum_{i=1}^{N} \frac{1}{{\omega_i}^2}\bar{\phi}_i\bar{\phi}_i^T \qquad \text{Eq. 9}$$

where M is the mass matrix, $\bar{\Phi} = [\bar{\phi}_1\ \bar{\phi}_2 \ldots \bar{\phi}_N]$ is the mode shape matrix, $\Omega = \text{diag}({\omega_i}^2)$ is the modal frequencies matrix (or spectral matrix), and N is the number of degrees of freedom (DOF) in the system. Any arbitrarily scaled or normalized mode shape ϕ_i is related to the mass-normalized mode as:

$$\bar{\phi}_i = \phi_i d_i \qquad \text{Eq. 10}$$

where d_i is a mass normalization constant for the i^{th} mode.

Suppose only a few (lower) modes are available, for example from experimental tests, a truncated flexibility matrix is obtained as:

$$F_{trun} = \sum_{i=1}^{n} \left(\frac{d_i}{\omega_i}\right)^2 \bar{\phi}_i\,\bar{\phi}_i^T \qquad \text{Eq. 11}$$

where nn is the number of modes available.

Let's define the difference (ΔF_{trun}) between the flexibility matrices of the true (damaged) structure and the trial FE model as:

$$\Delta F_{trun} = F_{trun}^{true} - F_{trun}^{trial} \qquad \text{Eq. 12}$$

When a trial FE model reasonably resembles the damaged structure with true damage, the difference in flexibility matrices is close to zero (exactly zero if there is no measurement noise nor modeling error). The scalar magnitude on the difference in the flexibility matrices can be measured by calculating the Frobenius norm of ΔF_{trun}:

$$\|\Delta F_{trun}\|_F = \sqrt{\sum_i \sum_j x_{ij}^2} \qquad \text{Eq. 13}$$

which vanishes when all matrix elements x_{ij} are zero (meaning the FEM model perfectly matches the observed structure).

The difference in the flexibility matrices can also be further decomposed into singular values by singular value decomposition (SVD):

$$\Delta F_{trun} = USV^T \qquad \text{Eq. 14}$$

where V^T and U are matrices of singular vectors, S is the diagonal matrix whose elements are the singular values, s_i. Since the Frobenius norm is invariant under unitary multiplication, the SVD of the ΔF_{trun} yields

$$\begin{aligned} \|\Delta F_{trun}\|_F &= \|USV^T\|_F \\ &= \|S\|_F \\ &= \sqrt{s_1^2 + s_2^2 + \cdots + s_R^2} \end{aligned} \qquad \text{Eq. 15}$$

where R is the rank of ΔF_{trun}.

Since the mode shapes experimentally obtained are arbitrary scaled, the mass normalization constants (d_i) are required to properly compute the flexibility matrix of the real, true structure. One approach to extracting the mass normalization constant is based on testing the structure with a perturbed mass matrix (by adding a known mass at a certain location) and examining the sensitivity of the eigenvalues [14, 15]. In this study, mass normalization constants estimated using the FEM model are updated at each trial and applied to the experimentally obtained (and not mass normalized) mode shapes. That is, the constants are extracted by comparing the mass-normalized mode shapes and displacement-normalized mode shapes, where both mode shapes are available as options in many commercial FEM programs (*e.g.*, ABAQUS).

EXPERIMENTAL TESTBED: ALUMINIUM PLATE WITH A WELDED STIFFNER

STRUCTURAL CHARACTERISTICS

The proposed Bayesian model-updating algorithm is applied to the problem of damage detection in a stiffened aluminum plate (Figure 2a). The design of this structural component is intended to include a geometric complexity that commonly found in aluminum ship hull structures. The aluminum plate includes an area with high stress concentration due to the presence of a welded stiffener. Such areas are likely locations for fatigue-related damage (*i.e.*, fatigue crack). Knowledge of this fact allows one to customize the model updating algorithm to prioritize the search of this area. The aluminum plate is 24 in by 48 in and is 0.249 in thick. In addition, the plate has a stiffener plate (2 in ×18 in × 0.249 in) and they are rigidly welded by a TIG weld. Three different crack paths initiating from the heat affected zone (HAZ) around the welded stiffener plate are considered as example damage scenario cases (Figure 2b).

The structural characteristics of the plate structure are first estimated using a general-purpose FEM analysis program (namely, ABAQUS). The base plate and stiffener plate are modeled with 4-node reduced integration, doubly curved shell elements with hourglass control (*S4RSW*) [16]. These plates are assumed to be rigidly connected. The mesh size of the plate elements are 1 in × 1 in. The elastic modulus of the undamaged (E) elements is 10300 ksi while for the cracked elements, the elastic modulus is reduced 10^{-6} times the original modulus ($E_d = E \times 10^{-6}$). The mass density of the aluminum is assumed to be 2.489×10^{-7} slug/in^3. The *Lanczos* frequency analysis method in ABAQUS provides the modal properties (*i.e.*, modal frequency and mode shape) of the base structure. For example, changes in the modal properties of the plate with the inclusion of a crack (path 1 in Figure 2b) are summarized in Table 1. The modal frequencies of the structure drop by 1 to 6% with noticeable decrease in the frequencies observed in the second to fourth modes. The changes in mode shapes are evaluated using the modal assurance criteria (MAC) (*i.e.*, the correlation between the undamaged and damaged mode shapes). Noticeable changes are observed for the higher modes (fourth and fifth modes) as intuitively expected.

EVALUATION OF THE OBJECT FUNCTIONS

The performances of the proposed objective (error) functions are evaluated using the crack paths shown in Figure 2b. Two necessary conditions of the objective functions are first tested. The first is the capability of the objective function to identify the starting location of crack path (*i.e.*, initial crack identification). The other condition is the monotonicity condition which states that the objective function monotonically decrease as the hypothesized cracked elements used in the trial model are increasingly included element by element along the true targeted damage path. The parameters considered when evaluating the objective functions are: 1) objective function type, 2) number of truncated modes, 3) location of the sensors (see Figure 3b), and 4) the location and size of the crack paths (see Figure 2b). Uncertainty in the measurement is not considered during these preliminary evaluations on the objective functions. The test parameters are summarized in Table 2.

Table 1. Changes in structural characteristics.

Modes (i)	1	2	3	4	5
Frequency (Hz): no crack	25.640	39.840	69.516	90.557	123.01
Frequency (Hz): cracked	25.302	38.049	67.620	85.364	121.09
Change in frequency (%)	-1.318	-4.495	-2.727	-5.735	-1.561
MAC (i, i)	0.997	0.999	0.997	0.924	0.960

Table 2. Performance tests of object functions.

Test Type	Object Function	Modes	Number of Sensors	Crack Path
MT, ICI	DMBA, FBA	1-5, 1-4, 2-5	6, 8, 12	1, 2, 3

MT: Monotonicity, ICI: Initial Crack Identification, DMBA: Direct Mode-Based Approach, FBA: Flexibility-Based Approach

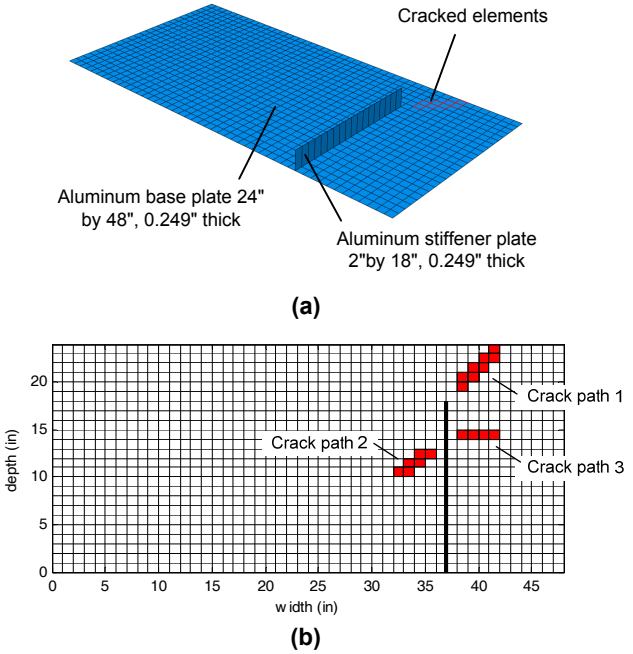

Figure 2. (a) Schematic of the base structure; (b) crack paths considered in analysis.

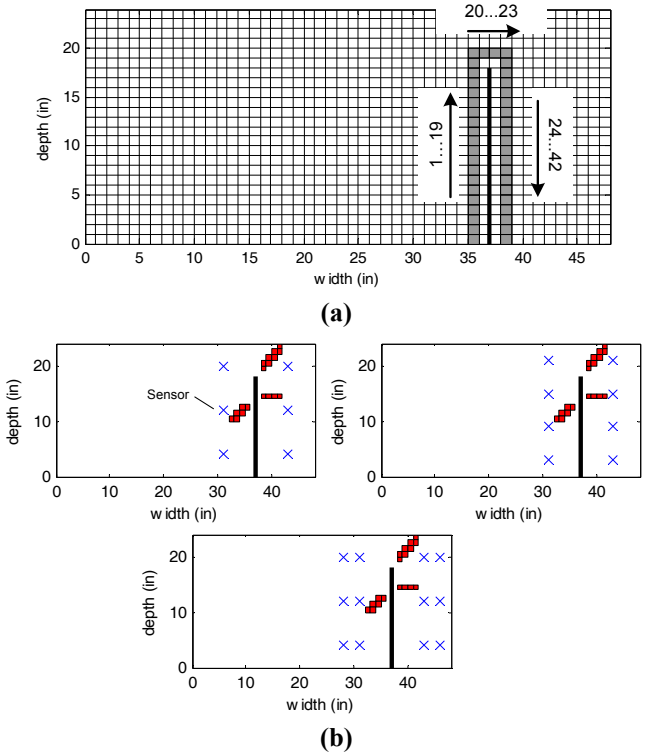

Figure 3. (a) Element number around the welds; (b) sensor locations.

The initial shape of the probability error distribution around the welded stiffener is first examined for the structure with no damage (Figure 4). Both the DMBA and FBA methods give similar error distributions with elevated errors at the location of element 20 (weld toe area; see Figure 3a for details). For Figure 4, the modes are truncated to consider the 2nd through 5th modes. As shown in Figures 4 and 5, the error distributions are sensitive to the inclusion of crack damages. In Figure 5, the DMBA method has a tendency to show small errors in the vicinity of the initiation of the crack paths (as denoted by the vertical dotted line in the plots). However, the method does not appear to be sensitive enough to identify the exact location of the true crack element (Figure 6). The truncation of modes does not affect the shape of the error distribution for the DMBA method. The FBA method shows an error function with a nearly concave shape which indicates a high probability for the existence of the true cracked element around the objective function minima. The concave shape becomes smoother and more obvious when the 1st mode is excluded in the calculation of the FBA objective function (*i.e.*, the case with the 2nd through 5th modes included). This result demonstrates, to some extent, that the FBA method has a better initial crack identification capability when compare to the DMBA method.

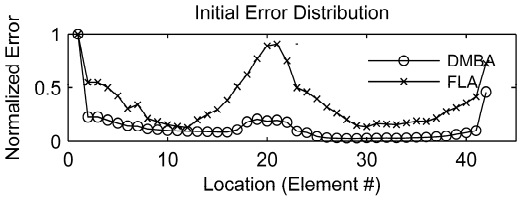

Figure 4. Initial error distribution around the stiffener weld.

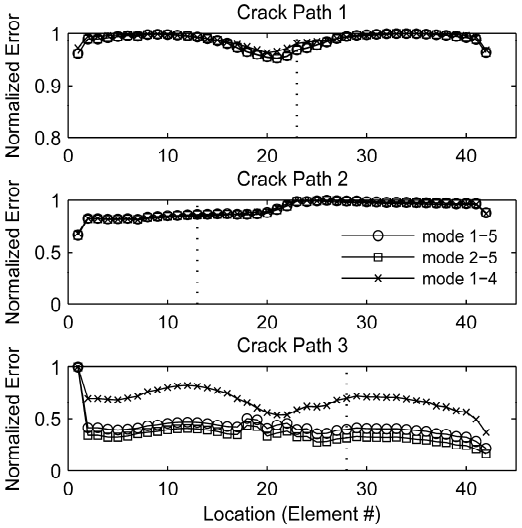

Figure 5. Error distribution around weld using the DMBA method.

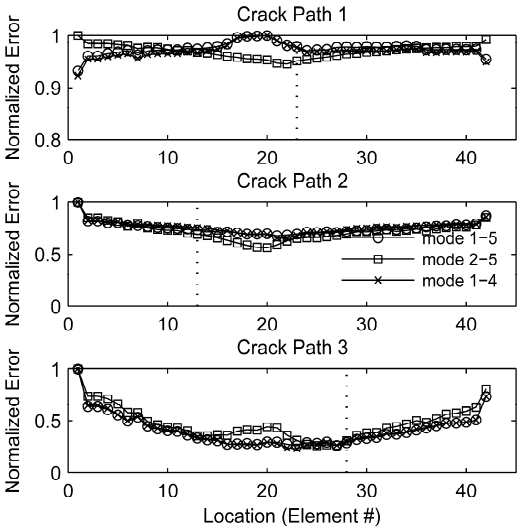

Figure 6. Error distribution around weld using the FBA method.

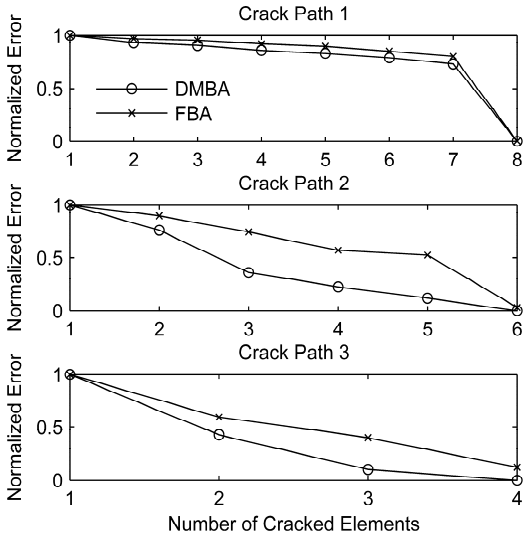

Figure 6. Monotonic decrease of error on crack path.

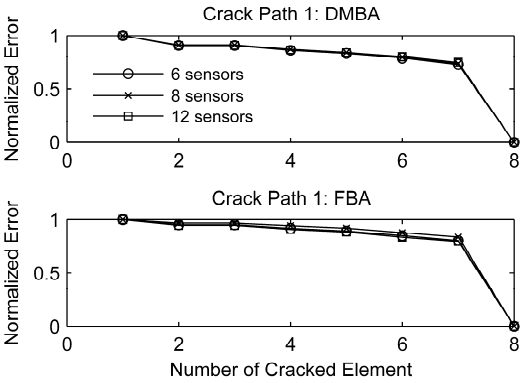

Figure 7. Effect of sensor locations in monotonicity condition.

The monotonicity condition is necessary to ensure that the Bayesian inference method increase in likelihood for the probable area of damage with trial (hypothesis). Figure 7 shows the strong monotonicity of the error function along all three crack paths considered in this study. Here, the number of cracked elements increases from the crack initiation on the weld side of the crack paths. For example, for crack path 1, there are 8 elements that have reduced Young's moduli corresponding to the simulated crack. The x-axis in Figure 7 represents the number of elements along the crack path used in the hypothesized model. In Figure 8, the sensitivity of the number of sensors on damage detection (see Figure 3b) is examined. As shown, the objective functions do not appear to exhibit sensitivity to the number of sensors used.

EXPERIMENTAL VALIDATIONS

TEST DESCRIPTIONS

The aluminum plate previously modeled in the numerical simulations was manufactured in full-scale to examine the performance of the proposed Bayesian damage detection algorithm in the noisy sensing environment common in real-life applications (Figure 9). A 18 in long stiffener plate was welded to the base plate with 1 in long discrete TIG welds at 5 locations (with a spacing of 3.6 in) to avoid excessive distortions that might result from weld heat. In addition, the base plate was pre-heated using a gas torch to increase the speed of the welding process. A simple straight cut was made by a vertical band saw to represent a fatigue crack in the base plate (Figure 9a). The base plate was fixed to stiff steel bars along the shorter edges of the plate using 8-3/8 in aluminum bolts. The assemblage was then rigidly connected to the concrete strong floor of the Structural Engineering Laboratory at the University of Michigan. A specimen without a crack was also prepared to estimate the material properties of the plates for the FEM model.

Two types of tests were conducted. One are modal hammer tests which a single input impact load at the center line of the specimen away from the weld and crack damage area (Figure 9b). The other tests use ambient excitations where the specimen is tapped by hands at random locations with quasi-random loads. The tests were repeated 3 and 5 times for the undamaged and cracked specimens, respectively (Table 3).

MODAL PROPERTIES

The impact hammer tests are used to identify the structure's modal properties. Impulse response functions can be converted to the frequency domain to obtain the frequency response functions of the plate. Figure 10 shows the Fourier spectra of the vertical acceleration responses measured at each sensor location for impact hammer tests (impacted at the plate center, see Figure 9c). The circles in the plots indicate the peaks identified in the spectrum. The modal frequencies identified repeatedly appeared in the spectra from test to test (Table 4). The modes involving torsional movement (*e.g.*, the second, fourth and fifth modes) were excited only at the edge of

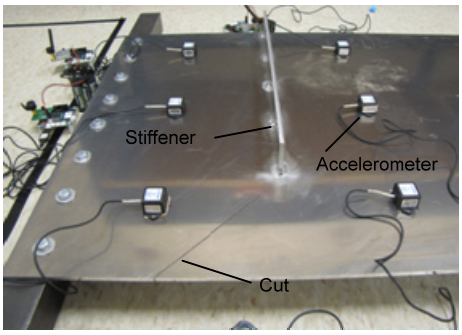

(a)

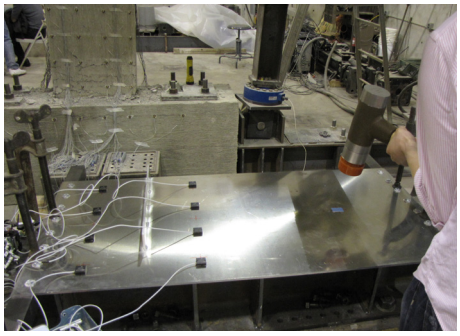

(b)

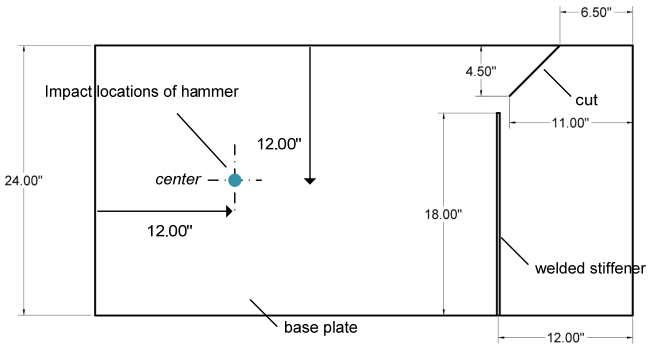

(c)

Figure 9. (a) Test specimen; (b) test view; (c) dimension of specimen.

Table 3. Test protocol.

Name	Type	Spec.	# of Sensor	Impact Location	Times
IH1C	hammer	cracked	6	center	5
IH2C	hammer	cracked	8	center	5
H1C	hand	cracked	6	random	5
H2C	hand	cracked	8	random	5
IH1N	hammer	no crack	6	center	3
IH2N	hammer	no crack	8	center	3
H1N	hand	no crack	6	random	3
H2C	hand	no crack	8	random	3

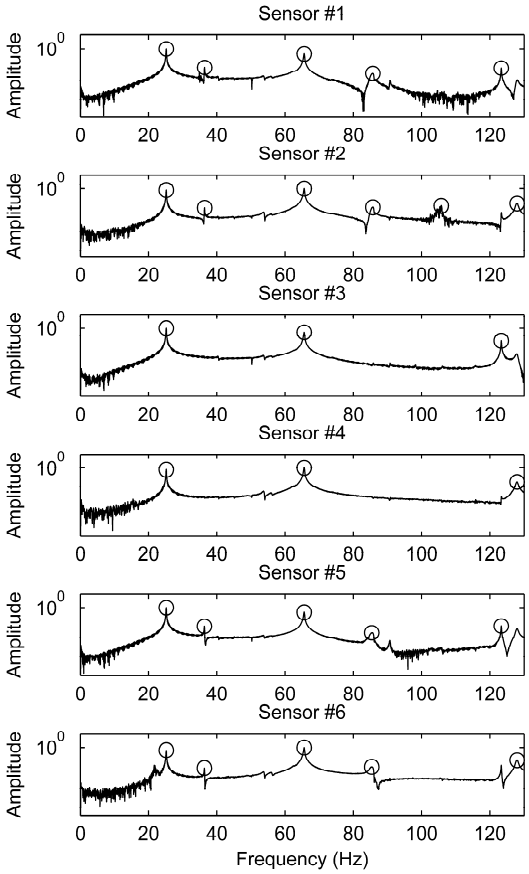

Figure 10. Fourier spectra of vertical vibrations at sensor nodes 1 through 6

the plate, and thus were hardly identified at sensors positioned at the center of the plate (*e.g.*, node 3 and 4). This led to lower periodicity numbers for those modes. Table 5 summarizes the modal frequency estimates for the cracked specimen in terms of mean values, standard deviations and periodicity. For the hand tapping tests, the estimated frequencies were almost equal to those obtained from the impact hammer tests.

BASE MODEL TUNING

The nominal structural properties assigned in the FE model (*i.e.*, plate thickness, Young's modulus) were updated before the application of the proposed Bayesian model updating algorithm used for damage detection. The thickness of the base plate and the stiffener plate both measured 0.241" (the nominal value was 0.249"). Using the test results from the undamaged specimen, the Young's modulus of the plates in their undamaged state was estimated to be 91% of the nominal value while the density of the aluminum plate was assumed to be the nominal value. A series of parametric analyses were conducted to achieve minimal modal errors. The mode shapes of the updated undamaged plate model are compared to the mode shapes experimentally obtained in Figure 11. Excellent agreement exists in all five modes. Table 6 summarizes the comparison between the FEM model and the undamaged plate.

Table 4. Modal frequency estimates for cracked specimen in the impact hummer tests (5 test runs)

Mode	Mean Frequency (Hz)	Standard Deviation	Periodicity (%)
1	25.21	0.000	100
2	36.41	0.031	70
3	65.61	0.000	100
4	85.50	0.180	50
5	123.37	0.027	80

Table 5. Modal frequency estimates for cracked specimen in hand tapping tests (3 test runs)

Mode	Mean Frequency (Hz)	Standard Deviation	Periodicity (%)	From Hammer test (%)
1	25.12	0.018	100	0.357
2	36.33	0.017	77.8	0.220
3	65.61	0.021	100	0.000
4	85.99	0.021	55.6	-0.573

Table 6. Modal frequency estimates

Mode	Modal frequency			MAC
	Test (Hz)	FEM (Hz)	Diff (%)	(%)
1	25.21	25.167	-0.161	0.9976
2	36.41	37.893	3.840	0.9826
3	65.61	67.362	2.597	0.992
4	85.50	85.135	-0.656	0.982
5	123.37	120.43	-2.426	0.9318

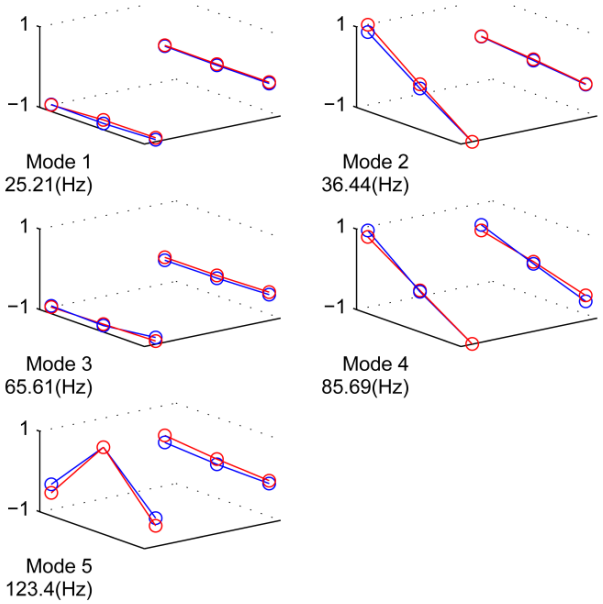

Figure 11. Mode shape comparison between impact hummer test results and FE model prediction

DAMAGE DETECTION

The proposed Bayesian model updating algorithm was applied to detect the damaged area in the test specimen. The modal properties of the specimen were estimated using the results from the impact hammer tests. The objective functions were formulated using the DMBA and FBA methods. The 2nd through 5th modes were considered in the truncated analyses. The initial hypothesized area of damage was the location in the vicinity of the stiffener weld. The analyses were repeated for three different pruning ratios applied in the BB pruning process (*i.e.*, 33.3%, 50% and 76.7%). The pruning process followed the branching of the survived candidate subsets. The approximate time durations of the Bayesian damage detection analyses with DMBA methods were 30 min, 2 h 30 min, and 14 h 20 min for the pruning ratios of 33.3%, 50% and 76.7%, respectively. With the FBA method, the analyses took 1 h 10 min, 6 h 50 min, and 47 h 30 min for the pruning ratios of 33.3%, 50% and 76.7%, respectively.

Figure 12 shows the histogram for the probable damage location for two objective functions (*i.e.,* DMBA and FBA). The appearances of each element were counted in the candidate subsets survived in each pruning process. The rule for the counting process was as follows: for an *N*-length candidate (*i.e.*, a candidate subset with *N* cracked elements), *i* th element was counted for *i* times so that elements positioned close to and far from the initial search area were equally evaluated for their appearances. In the histogram plots, the elements filled with darker color posses higher probabilities of damage (in this case, crack damage).

The DMBA method did not perform well and the probable damaged area was dispersed far away from the cracked elements (e.g., true crack path was pruned at the 4th branching process when the pruning ratio was 33.3%). The area of the probable damage became narrower as the pruning ratio increased. The FBA method successfully identified the damaged location in the vicinity of the true crack path (*e.g.*, true crack path was ranked as the 3rd among all candidate solutions when the pruning ratio was 33.3%). The elements colored dark correlated well with the location of the true crack even with large pruning ratios (*e.g.*, 76.7%). This fact indicated that with the selection of appropriate objective functions, significant computational time could be easily saved without sacrificing accuracy of the damage detection method.

CONCLUSIONS

The proposed Bayesian model updating method provides a probabilistic methodology for evaluating hypothesized damage states of an analytical model based on the use of measurement data. In addition, a Branch and Bound (BB) search method is used to prune the model state space resulting in significant speed-up in its execution. At the core of the Bayesian model updating method is the use of an objective function that evaluates how close a hypothesized model output is relative to the measurement data obtained from the real structure. In this study, two objective functions were considered including the

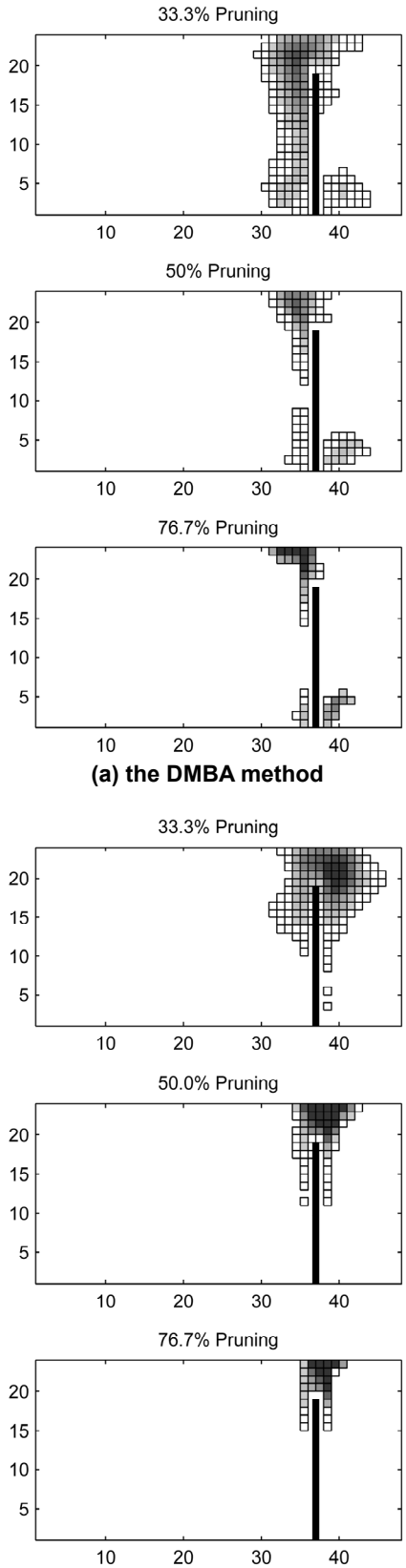

(a) the DMBA method

(b) the FBA method

Figure 12. Probable area of damage.

direct mode based approach (DMBA) and the flexibility based approach (FBA). The proposed algorithm was used to detect fatigue crack damage in an aluminum plate reinforced by a stiffener element welded to its top surface. Based on the experimental results obtained, the FBA objective function proved more accurate at hypothesizing the correct location of crack damage. The FBA method proved effective even when large pruning rates were adopted as a way of attaining computational speed-up. The authors will continue to investigate the performance of the Bayesian model updating algorithm with various objective functions. Furthermore, more complex aluminum hull sub-assemblages will also be tested under varying crack damage cases to assess the effectiveness of the method.

ACKNOWLEDGMENTS

The authors would like to gratefully acknowledge the support offered by the Office of Naval Research under Contract Numbers N00014-09-1-0567 and N00014-10-1-0613 awarded to University of Michigan and N00014-10-1-0384 awarded to Stanford University. The advice and suggestions offered by Dr. Paul Hess are also gratefully acknowledged.

REFERENCES

[1] Hoon, S., and Law, K.H., 2002, "A Bayesian Probabilistic Approach for Structure Damage Detection," *Earthquake Engineering and Structural Dynamics*, 26, pp. 1259-1281.

[2] Vanik, M.W., Beck, J.K., and Au, S.K., 2000, "Bayesian Probabilistic Approach to Structural Health Monitoring," *Journal of Engineering Mechanics*, 126(7), pp. 738-745.

[3] Cheung, S.H., and Beck, J.L., 2009, "Bayesian Model Updating Using Hybrid Mote Carlo Simulation with Application to Structural Dynamic Models with Many Uncertain Parameters," *Journal of Engineering Mechanics-ASCE*, 135(4), pp. 243-255.

[4] Stull, C.J., Earls, C.J., and Koutsourelakis, P-S., 2009, "Model-Based Structure Health Monitoring Using Parallel Stochastic Search Methods to Enable Inverse Solutions," *Proceedings of the 7th International Workshop on Structural Health Monitoring*, Stanford University, CA, pp. 1959-1969.

[5] Nichols, J.M., Link, W.A., Murphy, K.D., Olson, C.C., Bucholtz, F., and Mchalowicz, J.V., 2009, "A Bayesian Approach to Identifying and Tracking Damage in Structures," *Proceedings of the 7th International Workshop on Structural Health Monitoring*, Stanford University, CA, pp. 1951-1958.

[6] Norkin, V.I., Pflug, G. Ch., and Ruszczynski, A., 1998, "A Branch and Bound Method for Stochastic Global Optimization," *Mathematical Programming: Series A and B*, 83(3), pp. 425-450.

[7] Doebling, S. W., Farrar, C. R., and Prime, M. B., 1998, ''A Summary Review of Vibration-Based Damage Identification Methods". *The Shock and Vibration Digest*, 30, pp. 91-105.

[8] Chakraverty, S., 2008, "Vibration of Plates," CRC Press, Taylor & Francis Group, Boca Raton, FL.

[9] Pandey, A.K., and Biswas, M., 1994, "Damage Detection in Structures Using Changes in Flexibility," *Journal of Sound and Vibration*, 169(1), pp. 3-17.

[10] Pandey A.K., and Biswas, M., 1995, "Experimental Verification of Flexibility Difference Method for Locating Damage in Structures," *Journal of Sound and Vibration*, 184(2), pp. 311-328.

[11] Gao Y., and Spencer, B.F., Jr., 2002, "Damage Localization Under Ambient Vibration Using Changes in Flexibility," *Earthquake Engineering and Engineering Vibration*," 1(1), pp. 136-144.

[12] Bernal, D., 2006, "Flexibility-Based Damage Localization from Stochastic Realization Results," *Journal of Engineering Mechanics*, 132(6), pp. 651-658.

[13] Zonta D., Bernal D., 2006, "Strain-Based Approaches to Damage Localization in Civil Structures," *Proc. XXIV International Modal Analysis Conference*, Saint Louis, Mo, on CD.

[14] Brinker, R., and Anderson, P., 2002, "A Way of Getting Scaled Mode Shapes in Output-Only Modal Testing," *Proceedings of 21st Modal Analysis Conference (IMAC XXI),* Orlando, FL.

[15] Parloo, E., Verboven, P., Cuillame, P., and Overmeire, M.V., 2002, "Sensitivity-based Operational Mode Shape Normalization," *Mechanical Structures and Signal Processing*, 16(5), pp. 757-767.

[16] ABAQUS, 2010, "ABAQUS Analysis User's Manual," Dassault Systèmes, France.

